

AFRL-SN-WP-TP-2007-102

**HIGH-CYCLE LIFE TESTING OF RF
MEMS SWITCHES (PREPRINT)**

C.L. Goldsmith, D.I. Forehand, Z. Peng, and J.C.M. Hwang



DECEMBER 2006

Approved for public release; distribution unlimited.

STINFO COPY

This work was funded in whole or in part by Department of the Air Force contract F33615-03-C-7003. The U.S. Government has for itself and others acting on its behalf an unlimited, paid-up, nonexclusive, irrevocable worldwide license to use, modify, reproduce, release, perform, display, or disclose the work by or on behalf of the U.S. Government.

**SENSORS DIRECTORATE
AIR FORCE RESEARCH LABORATORY
AIR FORCE MATERIEL COMMAND
WRIGHT-PATTERSON AIR FORCE BASE, OH 45433-7320**

NOTICE AND SIGNATURE PAGE

Using Government drawings, specifications, or other data included in this document for any purpose other than Government procurement does not in any way obligate the U.S. Government. The fact that the Government formulated or supplied the drawings, specifications, or other data does not license the holder or any other person or corporation; or convey any rights or permission to manufacture, use, or sell any patented invention that may relate to them.

This report was cleared for public release by the Air Force Research Laboratory Wright Site (AFRL/WS) Public Affairs Office (PAO) and is available to the general public, including foreign nationals. Copies may be obtained from the Defense Technical Information Center (DTIC) (<http://www.dtic.mil>).

AFRL-SN-WP-TP-2007-102 HAS BEEN REVIEWED AND IS APPROVED FOR PUBLICATION IN ACCORDANCE WITH ASSIGNED DISTRIBUTION STATEMENT.

**//Signature//*

JOHN L. EBEL
Devices for Sensing Branch
Aerospace Components Division

//Signature//

KENICHI NAKANO, Chief
Devices for Sensing Branch
Aerospace Components Division

//Signature//

TODD A. KASTLE, Chief
Aerospace Components Division
Sensors Directorate

This report is published in the interest of scientific and technical information exchange and its publication does not constitute the Government's approval or disapproval of its ideas or findings.

Disseminated copies will show “//signature//*” stamped or typed above the signature blocks.

REPORT DOCUMENTATION PAGE

Form Approved
OMB No. 0704-0188

The public reporting burden for this collection of information is estimated to average 1 hour per response, including the time for reviewing instructions, searching existing data sources, gathering and maintaining the data needed, and completing and reviewing the collection of information. Send comments regarding this burden estimate or any other aspect of this collection of information, including suggestions for reducing this burden, to Department of Defense, Washington Headquarters Services, Directorate for Information Operations and Reports (0704-0188), 1215 Jefferson Davis Highway, Suite 1204, Arlington, VA 22202-4302. Respondents should be aware that notwithstanding any other provision of law, no person shall be subject to any penalty for failing to comply with a collection of information if it does not display a currently valid OMB control number. **PLEASE DO NOT RETURN YOUR FORM TO THE ABOVE ADDRESS.**

1. REPORT DATE (DD-MM-YY) December 2006		2. REPORT TYPE Conference Paper Preprint		3. DATES COVERED (From - To) 03/01/2006 – 09/01/2006	
4. TITLE AND SUBTITLE HIGH-CYCLE LIFE TESTING OF RF MEMS SWITCHES (PREPRINT)				5a. CONTRACT NUMBER F33615-03-C-7003	
				5b. GRANT NUMBER	
				5c. PROGRAM ELEMENT NUMBER 63739E	
6. AUTHOR(S) C.L. Goldsmith and D.I. Forehand (MEMtronics Corporation) Z. Peng and J.C.M. Hwang (Lehigh University)				5d. PROJECT NUMBER ARPS	
				5e. TASK NUMBER ND	
				5f. WORK UNIT NUMBER AN	
7. PERFORMING ORGANIZATION NAME(S) AND ADDRESS(ES) MEMtronics Corporation 3000 Custer Road Plano, TX 75075-4422				8. PERFORMING ORGANIZATION REPORT NUMBER Lehigh University Bethlehem, PA 18015	
9. SPONSORING/MONITORING AGENCY NAME(S) AND ADDRESS(ES) Sensors Directorate Air Force Research Laboratory Air Force Materiel Command Wright-Patterson Air Force Base, OH 45433-7320				10. SPONSORING/MONITORING AGENCY ACRONYM(S) AFRL-SN-WP	
				11. SPONSORING/MONITORING AGENCY REPORT NUMBER(S) AFRL-SN-WP-TP-2007-102	
12. DISTRIBUTION/AVAILABILITY STATEMENT Approved for public release; distribution unlimited.					
13. SUPPLEMENTARY NOTES Conference paper submitted to the Proceedings of the 2007 IEEE MTTTS IMS, published by IEEE. This work was funded in whole or in part by Department of the Air Force contract F33615-03-C-7003. The U.S. Government has for itself and others acting on its behalf an unlimited, paid-up, nonexclusive, irrevocable worldwide license to use, modify, reproduce, release, perform, display, or disclose the work by or on behalf of the U.S. Government. PAO Case Number: AFRL/WS 06-2917, 28 Dec 2006. Paper contains color.					
14. ABSTRACT RF MEMS capacitive switches capable of order of-magnitude impedance changes have demonstrated operating lifetimes exceeding 100 billion switching cycles without failure. In situ monitoring of switch characteristics demonstrates no significant degradation in performance and quantifies the charging properties of the switch silicon dioxide film. This demonstration lends credence to the mechanical robustness of RF MEMS switches.					
15. SUBJECT TERMS Microwave switches, RF MEMS					
16. SECURITY CLASSIFICATION OF:			17. LIMITATION OF ABSTRACT: SAR	18. NUMBER OF PAGES 10	19a. NAME OF RESPONSIBLE PERSON (Monitor) John Ebel
a. REPORT Unclassified	b. ABSTRACT Unclassified	c. THIS PAGE Unclassified			

High-Cycle Life Testing of RF MEMS Switches

C.L. Goldsmith¹, D.I. Forehand¹, Z. Peng², J.C.M. Hwang², and John L. Ebel³

¹MEMtronics Corporation, Plano, TX, USA, ²Lehigh University, Bethlehem, PA, USA

³Air Force Research Laboratory, Dayton, OH, USA

Abstract — RF MEMS capacitive switches capable of order-of-magnitude impedance changes have demonstrated operating lifetimes exceeding 100 billion switching cycles without failure. In situ monitoring of switch characteristics demonstrates no significant degradation in performance and quantifies the charging properties of the switch silicon dioxide film. This demonstration leads credence to the mechanical robustness of RF MEMS switches.

Index Terms — RF MEMS, reliability, dielectric charging, MEMS switches.

I. INTRODUCTION

MEMS switch technology has many potential benefits over conventional electronic devices for switching microwave and millimeter-wave signals. MEMS switches possess very low insertion loss, miniscule power consumption, and ultra-high linearity [1]. These characteristics make MEMS technology an ideal candidate for incorporation into passive circuits, such as phase shifters or tunable filters, for implementation in the passive front-end of phased antenna arrays at X-band and above.

With the excellent performance of electrostatically-operated, capacitive MEMS switches having been well-established with various component demonstrations, emphasis in RF MEMS research has shifted towards achieving a better understanding of MEMS switch reliability [2] and improving the packaging of MEMS switches. Efforts in the former have centered on methodologies to quantify the amount of charging present in capacitive MEMS switches, and relating that charging back to the electromechanics of the switch. In this manner, improvements in materials and mechanical designs can be quantified relative to increasing the operational lifetime of MEMS capacitive switches.

This paper delineates the electromechanical, RF, and charging properties of an “air-gap” capacitive switch, and shows how the switch can be utilized in high-cycle life testing. Monitoring both high-speed and low-speed switching characteristics provides valuable insight into quantifying the lifetime properties of the switch, and enable estimation of switching lifetime under a variety of operating conditions.

II. SWITCH CONSTRUCTION

Fig. 1 illustrates a state-of-the-art metal-dielectric-metal RF MEMS capacitive switch fabricated on a glass substrate. The processes used in the fabrication of this device are similar to

those reported in [1]. The top electrode is a 0.3- μm -thick flexible aluminum alloy membrane that is tied to DC and RF ground potential. The bottom switch electrode is composed of chromium/gold and serves as the center conductor of 50 Ω coplanar waveguide for the RF signal. Thick copper posts, approximately 3 μm tall, serve as the anchor points for the suspended MEMS membrane as well as the RF transmission line conductors. Without applied electrostatic force, the membrane is normally suspended in air 2.2 μm above the switch insulator. A control voltage in the range of 25-35 V, applied to the bottom electrode, pulls the membrane into contact with the dielectric thus forming a 120 μm x 80 μm capacitor to shunt the RF signal to ground. When the control voltage is removed, the membrane springs back to its fully suspended position due to the restoring force of the membrane, resulting in little capacitive loading of the RF line.

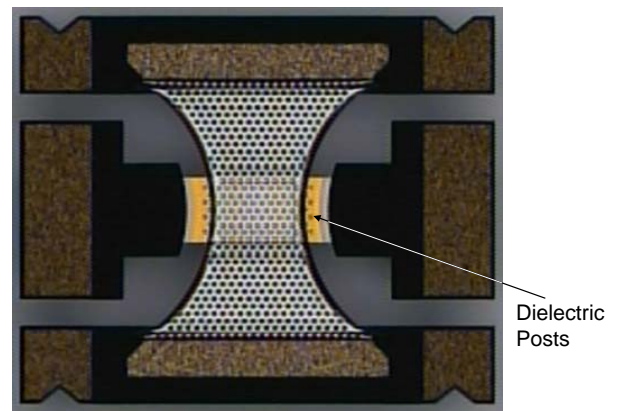


Fig. 1 - RF MEMS air-gap switch using patterned dielectric posts.

Within this switch, the layer of switch insulator is composed of sputtered silicon dioxide 0.28 μm thick ($\epsilon_r \sim 5.5$). The switch insulator is not a continuous sheet of dielectric, but patterned into a series of insulating, hexagonal posts approximately 4 μm across on an 8 μm pitch. The patterned dielectric bumps to create an “air-gap” or “proximity” switch, in which a larger percentage of the switch area utilizes air insulator rather than silicon dioxide. This use of patterned dielectric posts reduces the contact area accessible to dielectric charging. Trading off on-capacitance for reduced charging provides the opportunity for switching of moderate capacitance ratios (more like a switched reactance than a high isolation switch) with increased switch longevity.

III. SWITCH CHARACTERIZATION

Prior to the start of life testing, a thorough characterization of the electromechanical, RF, and dielectric charging performance was completed.

A. Electromechanical Performance - The bistable switching characteristics of the MEMS devices were tested by probing the switches with a swept voltage through a capacitance meter. An HP 33220A arbitrary waveform generator, driving a Tabor 9100 high-voltage amplifier, provided voltage drive to a Boonton 7200 capacitance meter, with its analog output captured and digitized using a Tektronix 2440 oscilloscope. These measurements were taken at multiple locations across the wafer. The average pull-in voltage was 30.1 volts with a standard deviation of 3.8 volts. The release voltage of the switches was measured to be approximately 17 volts. A typical operating curve of the MEMS proximity switch is shown in Fig. 2 below.

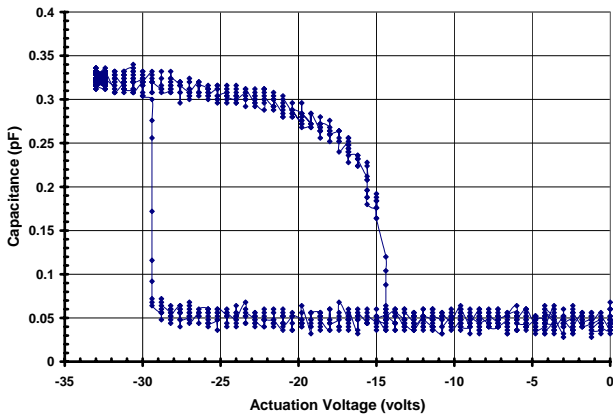


Fig. 2 - Dynamic operating curve for the MEMS proximity switch.

B. RF Properties - From the switch operating curves and appropriate test structures, the RF capacitive characteristics of the MEMS switch were extracted. The switch itself averages 44 fF of shunt off-capacitance, of which approximately 30 fF is plate capacitance and 14 fF is fringing capacitance. This switch capacitance is partially compensated with inductive feedlines in and out of the switch, yielding an effective shunt capacitance of ~ 15-20 fF in off-state. In the on-state, the proximity switch described above possesses 0.28 pF to 0.34 pF of on-capacitance. In a 50 ohm system, this switch provides a reactance ratio, approximately (280 ff to 340 ff) / (15 ff to 20 ff), in the range of 15:1 to 20:1.

The RF properties of these switches at microwave and millimeter-wave frequencies were measured on a HP 8510 vector network analyzer. The RF insertion loss of the MEMS switch is typical of most modern MEMS switches, with less than 0.1 dB insertion loss through 40 GHz. The magnitude of insertion loss and return loss of the proximity switch are presented in Fig. 3.

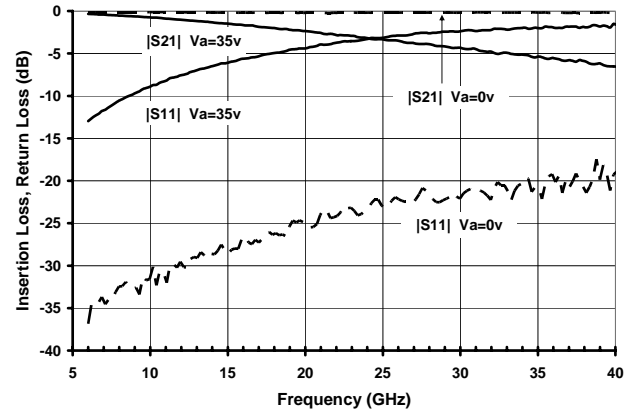


Fig. 3 - MEMS proximity switches possess excellent insertion loss and switched reactances of > 10:1.

C. Dielectric Charging Characterization - The characterization of switch insulator materials, specifically silicon dioxide, has improved in recent years with the application of transient current spectroscopy methods [3]. The model for this charging as a function of time is given by

$$Q = \sum_J Q^J \cdot [1 - \exp(-t_{ON} / \tau^J)] \cdot \exp[-t_{OFF} / \tau^J] \quad (1)$$

Where the time dependence of the charging behavior is approximated by the sum of two exponential terms ($J=1,2$), t_{on} and t_{off} being the on and off-times of applied voltage, τ the charging and discharging time constants (approximately equal), and Q^J the steady state charge density. The voltage dependence of the steady state charge density can be fitted by

$$Q^J = Q_0^J \exp(V / V_0) \quad (2)$$

Where V is the applied control voltage, and Q_0 and V_0 are the fitted parameters. The transient current measurements were made over a voltage range of 30-60 volts to quantify the change density as a function of both time and voltage. These techniques were applied to the sputtered silicon dioxide with the results provided in Table 1.

Table 1 - Silicon Dioxide Charging Characteristics

Negative Bias			
J	τ (sec)	Q_0 (cm ⁻²)	V_0 (volts)
1	5	2×10^{10}	16
2	52	6×10^{10}	16

This characterization was only completed for negative polarity, as this material commonly exhibits significantly higher charging for a positive polarity drive voltage. The test devices used for this characterization were MIM capacitors fabricated on the same wafers as the MEMS switches. Past work has shown that these measurements are good approximations to the charging occurring in real switches.

IV. DIELECTRIC CHARGING REDUCTION

The simple and most effective methods for reducing dielectric charging within MEMS switches are to reduce the operating voltage, reduce the dielectric area, and/or reduce the operating duty cycle. In order to achieve high cycle lifetime, all three of these techniques were utilized to minimize the amount of dielectric charging present in the switch.

A. Reduced Operating Voltage - It has been known for some time that higher operating voltages exponentially decrease the operating lifetime of the switch [2]. The lower limit of operating voltage is determined by the minimum restoring force necessary to ensure that surface forces do not induce stiction of the switch membrane. Further, the minimum control voltage is also determined by the ability to achieve a repeatable tensile stress of the switch membrane during fabrication. Residual stress of aluminum films are dependent on the temperature history of the membrane prior to release. For the equipment set utilized to fabricate these switches, tensile stresses in the 100-150 MPa range are the minimum repeatable values. With the given switch dimensions, this yields switches with approximately 30 volts pull-in voltage.

B. Reduced Dielectric Area - Minimizing the dielectric contact area of MEMS switches is becoming more common as the difficulties of overcoming dielectric charging become evident. [4, 5]. By changing from a continuous sheet of dielectric beneath the switch to an array of posts, the active area for charging can be reduced. The dielectric posts of 4 μm diameter/8 μm pitch used in this switch has a fill factor of 25%, thereby reducing dielectric charging by 25%. This trades off switch capacitance for reduced charging and increased longevity.

C. Reduced Duty Cycle - In order to obtain high cycle counts in switch lifetime measurements, it is necessary to operate the switch as quickly as possible. With typical switching times of ~5-8 microseconds, operating at cycling frequencies above 50 kHz yields short on- or off-times, with most of the period spent in transit between the two states. These switches were operated at 60 kHz, with a cycle period of 16.7 μs . In this case, the effective duty cycle for on-time was on the order of 10%. Using Eqs (1) and (2), with the simulation techniques established in [6], the impact of duty factor on dielectric charging can be quantified. Using the model data of Table 1, the saturated (infinite time) charge density as a function of duty factor for this dielectric film is modeled as shown in Fig. 4. Operating at this high speed reduces the switch on-time to approximately 10% duty factor, and therefore reduces the induced charge collected in the insulator by a factor (roughly linear) of 0.129. Reducing the duty cycle in this way also affords the opportunity to ascertain the saturated charge density of the insulator film, a very useful figure of merit.

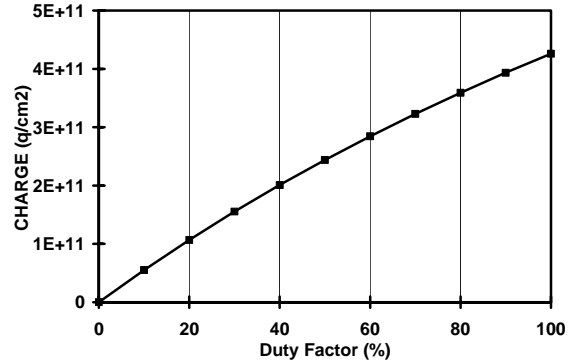


Fig. 4 - Modeled maximum charge density as a function of on-time duty factor for a capacitive MEMS switch built with the dielectric of Table 1.

V. RESULTS

A switch as described above was operated at -30 volts bias using a trapezoidal waveform at a repetition frequency of 60 kHz. The effective duty cycle of the switch was 10%. At this rate, the switch accumulated cycles at the rate of 216 million cycles/hr. The switch was run for a total of 476 hours without failure, accumulating a total of 102.8 billion cycles. During this process, snapshots of the slow-speed (1 kHz) and high speed (60 kHz) operating curves were recorded twice a day. The equipment and procedures for this characterization are given in [7]. The high-speed curves yielded information regarding operating at high cycling frequencies, while the slow-speed curves yielded diagnostic information regarding the pull-in and release voltages over the duration of the test.

From the high-speed operating curves, data points were accumulated at the minimum and maximum (fully up and fully down) states to determine if there was any drift in the RF performance of the device over the duration of the test. Fig. 5 displays the minimum and maximum RF detector signal for the duration of the test.

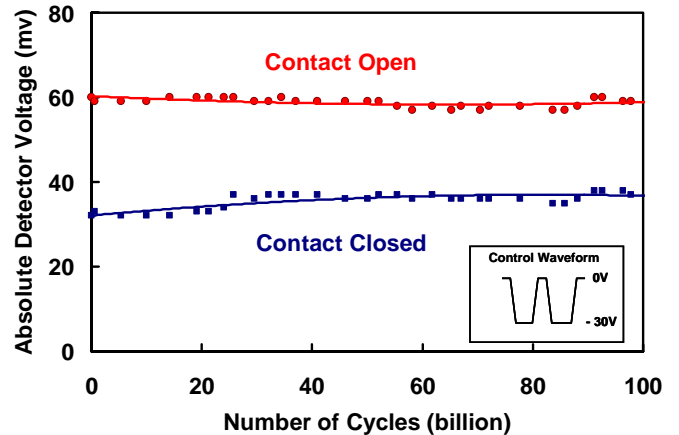


Fig. 5 - Isolation and insertion performance of switch during cycling.

VI. CONCLUSIONS

As can be seen in the figure, the off-state (contact up) was very stable over time. Though there was some drift in the on-state (contact down) detector signal over time, it is hard to quantify how much is generator or detector drift over the three weeks of testing. Qualitatively, there was no definitive degradation of the switch after accumulating the 100 billion cycles.

From the slow-speed operating curves, data points were accumulated to track the change in pull-in and release voltages. This provided information regarding the electromechanical performance and dielectric charging of the switch. Fig. 6 displays the extracted voltages as a function of accumulated cycles.

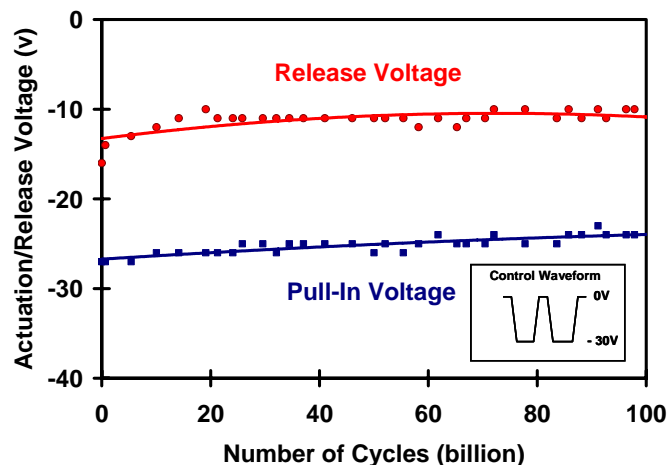


Fig. 6 - Diagnostic evaluation of switch operating parameters over cycle lifetime.

As can be seen from the graph, the change in pull-in and release voltages were monotonic over time (cycles). The total shift in pull-in voltage was 3 volts, while the total shift in release voltage was approximately 5 volts. Changes in pull-in voltage are likely a better metric of dielectric charging, as release voltages are also impacted by surface conditions of the switch [8].

The amount of charge accumulated during the 100 billion cycle test can be estimated as

$$\Delta V = hQ / \epsilon_R \epsilon_O \quad (3)$$

Where h is the effective height of a sheet of charge of density Q , within an insulator having a relative dielectric constant of ϵ_R . With h being approximately half the thickness of the dielectric film [3], 1400Å, this yields a saturated charge density of $6.5 \cdot 10^{15}$ carriers/cm².

Accounting for the dielectric fill factor and the operating duty factor, this equates to a maximum saturated carrier density of $2 \cdot 10^{17}$ carriers/cm² for a solid film of sputtered silicon dioxide operated under 100% duty cycle at -30 volts. This becomes a useful film figure-of-merit for estimating the performance of switches with differing fill factors or operating conditions.

While achieving 100 billion switching cycles without failure is a noteworthy achievement, it is important to understand how those results were achieved. Hero numbers for lifetime are too often obtained without providing insight into the mechanisms at play. These results pull together several years of development in quantifying dielectric charging, improving testing techniques, and designing for reduced dielectric charging. The results show that a switch capable of order-of-magnitude impedance change can operate for extended periods without charging-induced failure. It also demonstrates that the underlying mechanics of MEMS devices are robust and can cycle for extended periods.

In recent months, several switches, both packaged and unpackaged, have been tested beyond 100 billion cycles using the techniques put forth in this paper. These results have been achieved at three differing locations, Lehigh University, MEMtronics, and the Air Force Research Laboratory, with one switch achieving more than 200 billion cycles. Improved mechanical designs and innovative dielectric films are expected to enable even longer lifetimes in the near future.

ACKNOWLEDGEMENT

The authors appreciate the sponsorship of the Defense Advanced Research Projects Agency, for which this research was performed under Contract F33615-03-C-7003.

REFERENCES

- [1] Z.J. Yao, S. Chen, S. Eshelman, D. Denniston, and C. Goldsmith, "Micromachined low-loss microwave switches," *Journal of Microelectromechanical Systems*, vol. 8, no. 2, pp. 129-134, June 1999.
- [2] C. Goldsmith, J. Ehmke, A. Malczewski, B. Pillans, S. Eshelman, Z. Yao, J. Brank, and M. Eberly, "Lifetime Characterization Of Capacitive RF MEMS Switches," *2001 IEEE Int. Microwave Symp. Dig.*, vol. 1, pp. 227-230, May 2001.
- [3] X.B. Yuan, J.C.M. Hwang, D. Forehand, and C.L. Goldsmith, "Modeling and Characterization of Dielectric-Charging Effects in RF MEMS Capacitive Switches," *2005 IEEE Int. Microwave Symp. Dig.*, paper WE3B-3, June 2005.
- [4] C.L. Goldsmith, "Proximity Micromechanical Systems," *United States Patent 6,608,268*, issued August 19, 2003.
- [5] P. Blondy, A. Crunteanu, C. Champeaux, A. Catherinot, P. Tristant, O. Vendier, J.L. Cazaux, and L. Marchand, "Dielectric Less Capacitive MEMS Switches," *2004 IEEE Int. Microwave Symp. Dig.*, pp. 573-576, June 2004.
- [6] X.B. Yuan, Z. Peng, J.C.M. Hwang, D. Forehand, and C.L. Goldsmith, "A transient SPICE model for dielectric-charging effects in RF MEMS capacitive switches," *IEEE Trans Elect Dev*, Vol. 53, No. 10, pp. 2640-2648, Oct 2006.
- [7] C. Goldsmith, D. Forehand, X.B. Yuan, and J. Hwang, "Tailoring Capacitive Switch Technology for Reliable Operation," *2006 Govt Microcircuit Applications and Critical Tech Conf*, paper 2.01, pp. 1-4, San Diego, CA, Mar. 2006.
- [8] J.F. Kucko, J.C. Petrosky, J.R. Reid, and Y.K. Yeo, "Non-Charge Related Mechanism Affecting Capacitive MEMS Switch Lifetime," *IEEE Microwave Wireless Comp. Lett*, vol. 16, No. 3, pp. 140-142, Mar. 2006.